

# Automatic Change Detection for High-Resolution Satellite Images of Urban and Suburban Areas

Antigoni Panagiotopoulou, Lemonia Ragia

**Abstract**—High-resolution satellite images can provide detailed information about change detection on the earth. In the present work, QuickBird images of spatial resolution 60 cm/pixel and WorldView images of resolution 30 cm/pixel are utilized to perform automatic change detection in urban and suburban areas of Crete, Greece. There is a relative time difference of 13 years among the satellite images. Multiindex scene representation is applied on the images to classify the scene into buildings, vegetation, water and ground. Then, automatic change detection is made possible by pixel-per-pixel comparison of the classified multi-temporal images. The vegetation index and the water index which have been developed in this study prove effective. Furthermore, the proposed change detection approach not only indicates whether changes have taken place or not but also provides specific information relative to the types of changes. Experimentations with other different scenes in the future could help optimize the proposed spectral indices as well as the entire change detection methodology.

**Keywords**—Change detection, multiindex scene representation, spectral index, QuickBird, WorldView.

## I. INTRODUCTION

URBAN areas are the center of human habitation as well as of social and economic activities. As urban areas rapidly expand, any adjacent forest, cultivated land and water areas usually disappear. The latter causes problems in the environment, in the ecology as well as in resource management [1].

Remote sensing technologies and specifically high-resolution (HR) satellite images can be utilized to obtain urban and suburban information. Then, urban phenomena can be monitored and predicted while disaster response and sustainable development can be supported upon decision timely and efficiently [2]. Detection of urban targets such as buildings and water bodies or classification of urban land use/land cover can be followed by change detection to monitor the landscape. During change detection from HR images the basic challenge is the perplexity of radiometric and real semantic changes [3]. In multi-temporal HR images, the spectral signature of a certain object may vary at different dates due to several factors such as different imaging conditions, mis-registration and disparity of vertical structures broadly used.

Machine learning-based techniques for change detection [4] are additionally, automatic methods namely the pulse-coupled neural networks [5], the multi-temporal morphological

attribute profiles [6] and the multi-level change vector analysis [7] are widely met. Reference [8] utilizes basic urban primitives to get comparative information about blocks in the multi-temporal images. Then, the changed area and type can be pointed out. Also, a multi-level change detection approach can be found in [9].

In the present work multi-temporal QuickBird and WorldView images are utilized to perform automatic change detection in urban and suburban areas of Crete, Greece. The scene is classified into buildings, vegetation, water and ground by means of multiindex representation. In this study vegetation and water indices have been developed. After classification, the multi-temporal images get compared pixel-per-pixel and automatic change detection is performed.

Section II describes the remotely sensed imagery data. The methodology and the results are given in Section III while the conclusions are drawn in Section IV.

## II. SATELLITE IMAGE DATA

The experimental data consist of WorldView images of spatial resolution 30 cm/pixel and QuickBird images of 60 cm/pixel. The study area is Georgioupoli in the island of Crete, Greece [10]. Two different scenes near the shore have been selected for the current study. Actually, there is a time difference of 13 years among the satellite images. Figs. 1 and 2 depict the QuickBird and WorldView images, respectively, of “Scene 1”. Regarding “Scene 2”, the satellite images are shown in Figs. 3 and 4.

The spatial resolution [11] of QuickBird images has been increased per the factor of 2 by means of bicubic interpolation. Thus, all images that are depicted in Figs. 1-4 have the same spatial resolution equal to 30 cm/pixel. Also, the QuickBird images have been spatially or geometrically co-registered to the WorldView images. The WorldView images depict a more built-up area in relation to the QuickBird images, due to human intervention in the meantime.

The satellite images present four spectral bands, Table I. The WorldView image bands 2, 3, 4 and 5 correspond to the blue, green, yellow and red channels, respectively. As far as the QuickBird image is concerned, the bands 1, 2, 3 and 4 represent the blue, green, red and near-infrared channels, correspondingly.

TABLE I  
SATELLITE IMAGE BANDS

WorldView	QuickBird
2, 3, 4, 5	1, 2, 3, 4
Blue, green, yellow, red	Blue, green, red, near-infrared

A. Panagiotopoulou is with the University of Patras, Rio, 26504, Greece (corresponding author, e-mail: anpanag@upatras.gr).

L. Ragia is with the Information Management Systems Institute, Athena Research Center, Artemidos 6, Marousi 151 25, Greece (e-mail: leragia@athenarc.gr).



Fig. 1 QuickBird image of “Scene 1” at spatial resolution 30 cm/pixel after bicubic interpolation has been applied at the original one of resolution 60 cm/pixel



Fig. 2 WorldView image of “Scene 1” at spatial resolution 30cm/pixel. 13 years have passed from the “Scene 1” which is depicted in Fig. 1

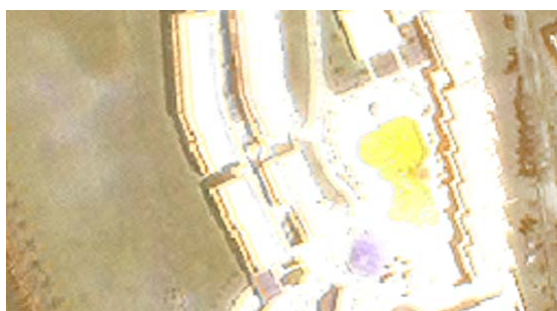


Fig. 3 QuickBird image of “Scene 2” at spatial resolution 30 cm/pixel after bicubic interpolation has been applied at the original one of resolution 60 cm/pixel

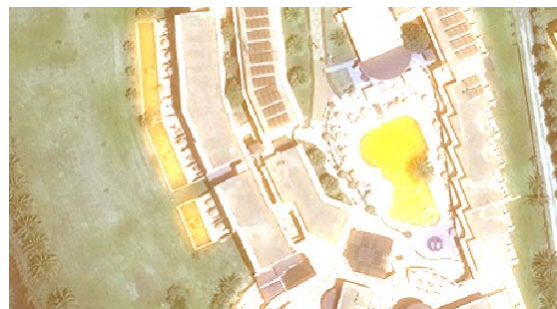


Fig. 4 WorldView image of “Scene 2” at spatial resolution 30 cm/pixel. 13 years have passed from the “Scene 2” which is depicted in Fig. 3

### III. METHODOLOGY AND RESULTS

#### A. Multiindex Scene Representation

Initially, multiindex scene representation [8] is applied on the images to classify the scene into buildings, vegetation, water and ground. Building detection is performed utilizing the morphological building index by the algorithm which is given in [12] and [13]. Regarding vegetation detection, the following spectral index is proposed:

$$VEG = B - 0.5G \quad (1)$$

where  $B$  denotes the blue channel radiance and  $G$  represents the green channel radiance. The vegetation signals get enhanced through the difference between blue and green bands. In fact, in a typical urban scene, soil shows a relatively low reflectance in the blue channel [8]. Reducing the effects of buildings and water using the green band, can lead to vegetation detection. The multiplicative factor 0.5 to the green channel is deemed necessary after experimentation.

Regarding water detection in the literature, identification of water body types from urban HR images is developed in [14]. In [15] a method for detection of open surface water in urbanized areas is presented. Inequality constraints and physical magnitude constraints serve for identification tools. Reference [16] detects water in urban area by GaoFen-3 synthetic aperture radar images. In [17] the problem of detecting swimming pools in QuickBird HR images of urban areas is addressed. Also, spectral indices for urban scene classification are presented in [18]. As far as the present study is concerned, for water body detection the spectral indices in (2) and (3) are proposed.

For the WorldView images:

$$WTR_1 = 3(G - Y) \quad (2)$$

For the QuickBird images:

$$WTR_2 = 3(G - R) \quad (3)$$

In (2)-(3), the symbols  $Y$  and  $R$  denote the yellow and red channel radiance, respectively. The difference between green and yellow bands or between green and red bands can enhance the water signals. Actually, soil presents a reflectance peak in

the yellow or red channel in urban scenes [8]. Since buildings are spectrally similar to the bright soil [8], reducing the effects of both soil and buildings using the yellow or red channel, can give the water detection. The multiplicative factor 3 in (2)-(3) is deemed necessary after experimentation.

The information maps of the images are depicted in Figs. 5-8. Red color denotes buildings, green color shows vegetation, blue is water while black represents soil and roads. The structural changes which have arisen from the QuickBird to the WorldView image are discernible in both scenes.

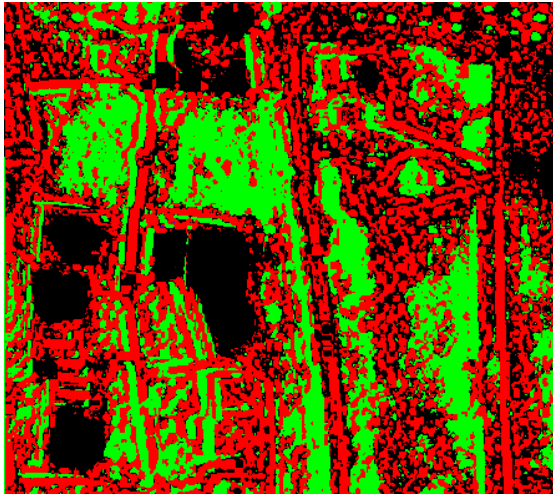


Fig. 5 Multiindex urban representation of QuickBird image of “Scene 1”: Red = buildings [12], [13], Green = Vegetation (proposed technique), Blue = water (proposed technique), Black = Ground (e.g., soil and roads)

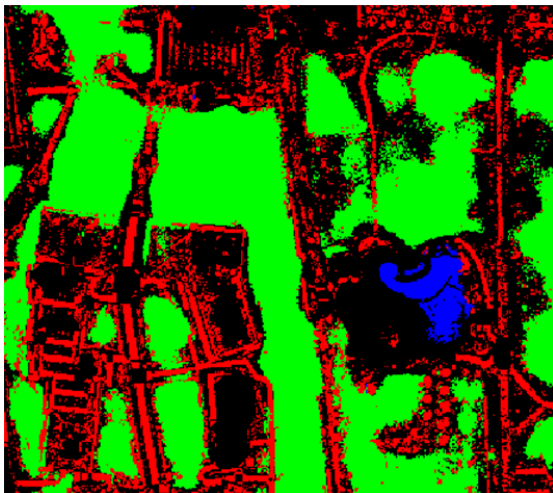


Fig. 6 Multiindex urban representation of WorldView image of “Scene 1”: Red = buildings [12], [13], Green = Vegetation (proposed technique), Blue = water (proposed technique), Black = Ground (e.g., soil and roads)

Figs. 9-12 depict the corresponding image-based histograms. According to the information maps and the related histograms, in “Scene 1” after 13 years the ground has increased per 12%, the water has increased per 1% and the vegetation has increased per 11%. Regarding the buildings,

these are detected to have decreased per 25%. As far as “Scene 2” is concerned, the information maps and the histograms show that after 13 years, buildings have decreased per 2%, vegetation has increased per 9%, water has increased per 3% but soil and roads have decreased per 9%. The above percentages can be found in accordance with visual inspection of Figs. 1-4.

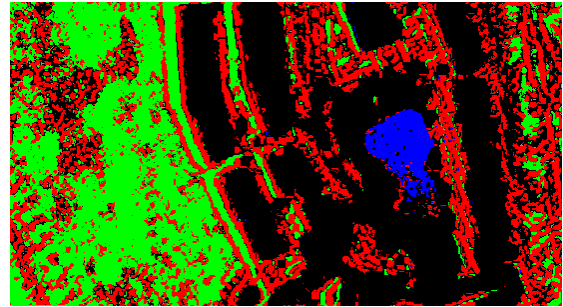


Fig. 7 Multiindex urban representation of QuickBird image of “Scene 2”: Red = buildings [12], [13], Green = Vegetation (proposed technique), Blue = water (proposed technique), Black = Ground (e.g., soil and roads)

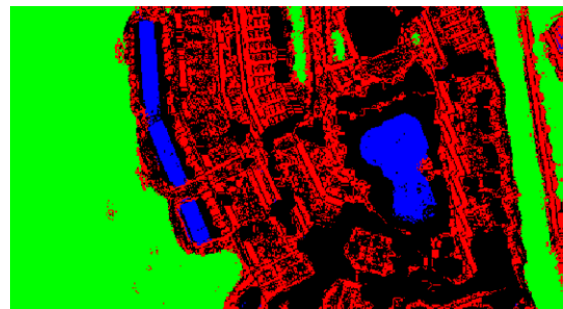


Fig. 8 Multiindex urban representation of WorldView image of “Scene 2”: Red = buildings [12], [13], Green = Vegetation (proposed technique), Blue = water (proposed technique), Black = Ground (e.g., soil and roads)

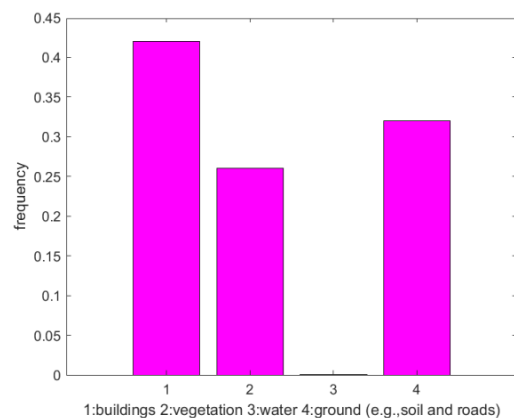


Fig. 9 Image-based histogram of QuickBird image of “Scene 1”

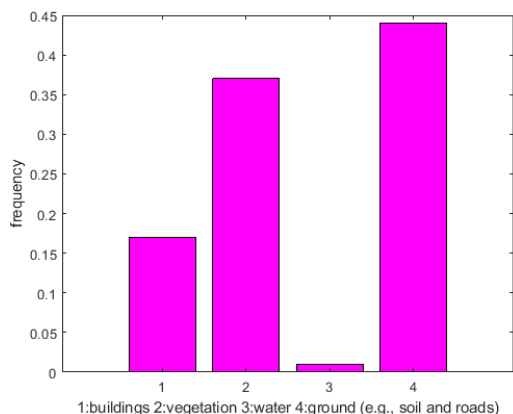


Fig. 10 Image-based histogram of WorldView image of “Scene 1”

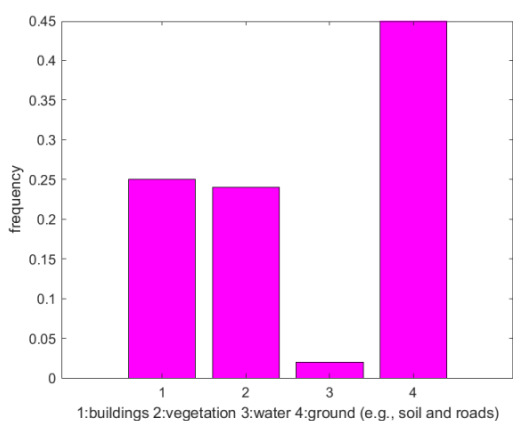


Fig. 11 Image-based histogram of QuickBird image of “Scene 2”

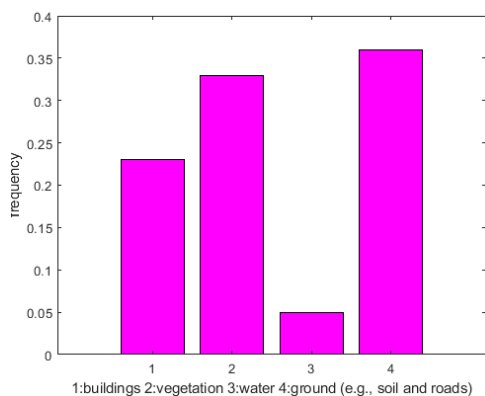


Fig. 12 Image-based histogram of WorldView image of “Scene 2”

### B. Change Detection

Automatic change detection is performed by pixel-per-pixel comparison of the classified multi-temporal images that are shown in Figs. 5-8. The results of the pixel-per-pixel comparison are depicted in Figs. 13 and 14 for the two scenes under study. Depending on the color of the change detection map, a different structural change has taken place. To be more specific, red, green and blue colors denote change in buildings, vegetation and water, respectively. Additionally, yellow color represents simultaneous change in buildings and vegetation while magenta color shows concurrent change in

buildings and water. As far as turquoise color is concerned, it denotes coincident change in vegetation and water. No change or ground is represented with black color. The proposed automatic change detection method not only indicates whether changes have taken place or not but also specifies the types of changes.

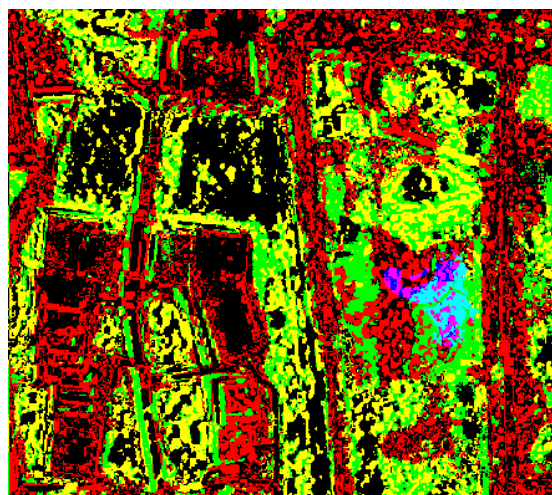


Fig. 13 Change detection from the QuickBird image to the WorldView image of “Scene 1” after 13 years have passed: Red = buildings, Green = vegetation, Blue = water, Yellow = buildings and vegetation, Magenta = buildings and water, Turquoise = vegetation and water, Black: no change or ground (proposed technique)

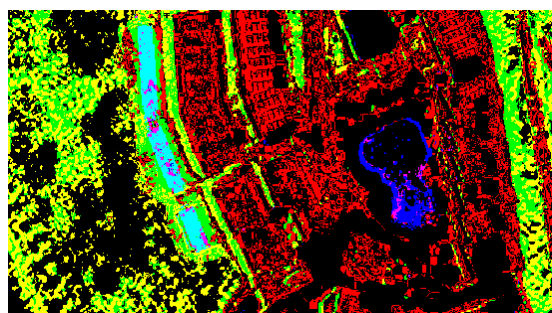


Fig. 14 Change detection from the QuickBird image to the WorldView image of “Scene 2” after 13 years have passed: Red = buildings, Green = vegetation, Blue = water, Yellow = buildings and vegetation, Magenta = buildings and water, Turquoise = vegetation and water, Black: no change or ground (proposed technique)

Change detection is also performed by means of the technique in [19]. This is an unsupervised change detection method. K-means clustering is performed on feature vectors which are extracted using local data projection onto eigenvector space, having been produced by principal component analysis. The results of change detection are depicted in Figs. 15 and 16 for both scenes. The technique in [19] indicates only whether changes have occurred or not. So, in Figs. 15 and 16 white color denotes change while black color means that no change has taken place. The particular algorithm takes as input the images of Figs. 1-4. However, the proposed change detection technique, whose results are illustrated in Figs. 13 and 14, needs as input the information

maps of Figs. 5-8. The change detection results which arise from the two different approaches, proposed one and that in [19], are not in full accordance.



Fig. 15 Change detection from the QuickBird image to the WorldView image of "Scene 1" after 13 years have passed: White = change, Black = no change [19]

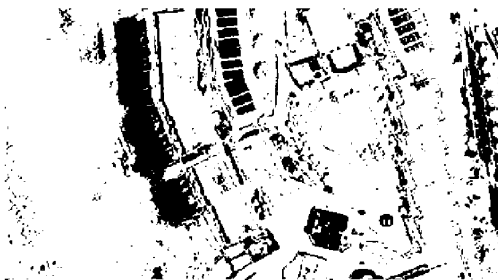


Fig. 16 Change detection from the QuickBird image to the WorldView image of "Scene 2" after 13 years have passed: White = change, Black = no change [19]

#### IV. CONCLUSIONS

In the present work, 4-channel QuickBird and WorldView images are utilized to perform automatic change detection in urban and suburban areas of Georgioupoli, in the island of Crete, Greece. There is a time difference of 13 years among the satellite images. The spatial resolution of QuickBird images has been increased per the factor of 2. So, all images that undergo processing have the same spatial resolution equal to 30 cm/pixel. Initially, the image scene is classified into buildings, vegetation, water and ground (i.e., soil and roads) by means of multiindex scene representation. Building detection is performed utilizing the already existing from the literature morphological building index. Regarding vegetation and water detection, these are performed by spectral indices which are proposed in the current study. Afterwards, automatic change detection is performed by comparing pixel-per-pixel the classified multi-temporal images. The proposed change detection methodology provides indication about whether changes have taken place or not and also gives specific information regarding the types of changes.

In future research, apart from bicubic interpolation, super-resolution techniques will be applied on the QuickBird images

so that to perform more accurate spatial resolution enhancement. Also, the use of public domain image datasets that contain ground-truth annotation could be considered for experimentation so that to better assess the advantages and disadvantages of the proposed methodology. Furthermore, the proposed change detection method along with the spectral indices will be validated in a greater number of urban and suburban areas than now with HR satellite images. Actually, routine urban monitoring could be an application of the proposed method. Additionally, the proposed method could be enriched and extended so that to also solve other scene-based image processing tasks such as content-based image retrieval and complicated pattern recognition.

#### REFERENCES

- [1] J. Gong, C. Liu, and X. Huang, "Advances in urban information extraction from high-resolution remote sensing imagery", *Sci. China Earth Sci.*, vol. 63, no. 4, pp. 463-475, Dec. 2020.
- [2] C. Marin, F. Bovolo, and L. Bruzzone, "Building change detection in multitemporal very high resolution SAR images", *IEEE Trans. Geosci Remote Sens.*, vol. 53, no. 5, pp. 2664-2682, May 2015.
- [3] L. Bruzzone and F. Bovolo, "A novel framework for the design of change-detection systems for very-high-resolution remote sensing images", *IEEE Proc.*, vol. 101, no. 3, pp. 609-630, March 2013.
- [4] M. Volpi, D. Tuia, F. Bovolo, M. Kanevski, and L. Bruzzone, "Supervised change detection in VHR images using contextual Information and support vector machines", *INT J APPL EARTH OBS*, vol. 20, pp. 77-85, Feb. 2013.
- [5] F. Pacifici and F. Del Frate, "Automatic change detection in very high resolution images with pulse-coupled neural networks", *IEEE Geosci. Remote Sens. Lett.*, vol. 7, no. 1, pp. 58-62, Jan. 2010.
- [6] N. Falco, M. D. Mura, F. Bovolo, J. A. Benediktsson, and L. Bruzzone, "Change detection in VHR images based on morphological attribute profiles", *IEEE Geosci. Remote Sens. Lett.*, vol. 10, no. 3, pp. 636- 640, May 2013.
- [7] F. Bovolo, "A multilevel parcel-based approach to change detection in very high resolution multitemporal images", *IEEE Geosci. Remote Sens. Lett.*, vol. 6, no. 1, pp. 33-37, Jan.2009.
- [8] D. Wen, X. Huang, L. Zhang, and J. A. Benediktsson, "A novel automatic change detection method for urban high-resolution remotely sensed imagery based on multiindex scene representation", *IEEE Trans. Geosci Remote Sens.*, vol. 54, no. 1, pp. 609-625, Jan. 2016.
- [9] X. Huang, D. Wen, J. Li, and R. Qin, "Multi-level monitoring of subtle urban changes for the megacities of China using high-resolution multi view satellite imagery", *Remote Sens. Environ.*, vol. 196, pp. 56- 75, Jul. 2017.
- [10] L. Ragia and P. Krassakis, "Monitoring the changes of the coastal areas using remote sensing data and geographic information systems", in *SPIE Proceedings of the Seventh International Conference RSCy2019*, Paphos, 2019, 111740X.
- [11] E. Bratsolis, A. Panagiotopoulou, M. Stefouli, E. Charou, N. Madamopoulos and S. Perantonis, "Comparison of optimized mathematical methods in the improvement of raster data and map display resolution of Sentinel-2 images", in *IEEE ICIP Proc.*, Athens, 2018, pp. 2521-2525.
- [12] X. Huang, W. Yuan, and L. Zhang, "A new building extraction postprocessing framework for high-spatial-resolution-remote-sensing-Imagery", *IEEE J Sel Top Appl Earth Obs Remote Sen*, vol. 10, no. 2, pp. 654-688, Febr. 2017.
- [13] X. Huang and L. Zhang, "A multidirectional and multiscale morphological index for automatic building extraction from multispectral GeoEye-1 imagery", *PE&RS*, vol. 77, no. 7, pp. 721-732, Jul. 2011.
- [14] X. Huang, C. Xie, X. Fang, and L. Zhang, "Combining pixel- and object-based machine learning for identification of water-body types from urban high-resolution remote-sensing imagery", *IEEE J Sel Top Appl Earth Obs Remote Sens*, vol. 8, no. 5, pp. 2097-2110, May 2015.
- [15] X. Liu, L. Liu, Y. Shao, Q. Zhao, Q. Zhang, and L. Lou, "Water detection in urban areas from GF-3", *Sensors*, vol. 18, no. 1299, pp.1-12, Apr. 2018.

- [16] F. Chen, X. Chen, T. Van de Voorde, D. Roberts, H. Jiang, and W. Xu, "Open water detection in urban environments using high spatial resolution remote sensing imagery", *Remote Sens. Environ.*, vol. 242, pp. 1-17, Jun. 2020.
- [17] C. Galindo, P. Moreno, J. Gonzalez, and V. Arevalo, "Swimming pools localization in colour high-resolution satellite images", in *IGARSS 2009*, CapeTown, pp. IV-510-IV513.
- [18] Mst I. Faridatul and B. Wu, "Automatic classification of major urban land covers based on novel spectral indices", *ISPRS Int. J. Geo- Inf.*, vol. 7, no. 453, pp. 1-25, Nov. 2018.
- [19] T. Celik, "Unsupervised change detection in satellite images using principal component analysis and k-means clustering", *IEEE Geosci. Remote Sens. Lett.*, vol. 6, no. 4, pp. 772-776, Oct. 2009.